Preliminary Geometry Analysis for Compact Scanning and Multi-Beam Reflectarray Antennas

Andrés Gómez-Álvarez, Álvaro F. Vaquero, Manuel Arrebola and Marcos R. Pino
Group of Signal Theory and Communications
Universidad de Oviedo
Gijón, Spain
Email: {andresga, fernandezvalvaro, arrebola, mpino}@uniovi.es

***Abstract*—This work presents a comparative study between two common compact configurations for reflectarray (RA) beam scanning in Ka-band: focal-arc and linear feed displacements. A reference phase-only design is defined for a collimated pattern, and the natural degradation caused by feed de-focusing is studied for each case. Practical considerations regarding the implementation of each solution are also discussed. Finally, the discrepancies between the presented phase-only study and a physical cell response are evaluated. A layout is defined, and its response is calculated for a set of feed positions considering the real incidence angles at each cell. These results are compared to the previous phase-only analysis.**

Keywords—compact mechanical beam scanning; multi-beam; reflectarray; Ka-band.

I. Introduction

High-throughput satellite communications in Ka-band have become increasingly important over the last years. These have pushed research for high-gain wide-angle beam scanning solutions for the ground segment. With electronically reconfigurable active arrays being prohibitively expensive at large scales, mechanical beam scanning based on passive reflectarray (RA) or transmitarray (TA) antennas proves to be a cost-effective low-loss alternative [1].

An important aspect of designing a RA-based mechanical scanning solution is defining the geometry to be used. Dual-RA designs are required for a true bi-focal solution [2], but the additional surface makes them bulky and heavy. Single-reflector designs optimized for a range of feed positions are a simpler and lighter alternative, albeit at the cost of lower scanning performance –mainly in terms of antenna gain and side lobe level (SLL). In this case, determining the optimal feed positioning and its displacement path is not trivial. This is not an issue in TA-based designs, where centered configurations are the norm [3]. When working with a reflector, beam blockage by the feed or its support structure can become a major problem. Feed positioning must therefore be considered, balancing any blocking degradations with other mechanical and performance requirements. This is particularly important for compact designs ($F/D < 0.5$), where the feed position is close to the RA surface. This work provides a preliminary analysis of the most common geometries used for RA-based mechanical scanning.

II. Design Principles

It is known from array theory that a collimated beam is achieved by generating a progressive phase distribution on the reflected fields over the reflectarray (RA) surface. For a feed radiating a spherical phase front, the phase shift that a point (x, y) on the array should introduce to the incident field to generate a beam towards (θ, φ) is given by:

$$\phi_{RA} = k_0\big(d - \sin\theta\,(x\cos\varphi + y\sin\varphi)\big) \qquad (1)$$

where d is the distance to the feed's phase center. From the incident fields and the phase response of the array, the reflected tangential fields are obtained. The far-field radiation diagrams can then be calculated by applying the second principle of equivalence at the reflector aperture [4].

When the feed is moved away from the focal point the reflectarray is defocused, changing the propagation delay to every point on the surface. As a result, the radiation diagram degrades, and the beam direction is shifted. This natural shift is the base for most mechanical beam scanning and multibeam RA designs based on feed displacements. Optimization on the array phase response distribution is required to equalize the beams within the desired scan range. The results that this optimization can achieve are however limited by the chosen geometry, e.g. how the feed is positioned and oriented for each radiation angle.

This work studies the natural scanning performance of common feed displacement geometries. The illuminated array is designed for a collimated beam using (1), and the natural degradation and scanning range is discussed for each case. Regarding the feeding element, an ideal x-polarized feed model is used based on the one proposed in [5]. For a (r, θ, φ) point expressed in the feed coordinate system (see Fig. 1), the radiated far-field is:

$$\vec{E} = E_0\,\frac{k_0}{2\pi r}\,e^{-jk_0 r}\big(\cos\varphi\,\hat{\theta} - \sin\varphi\,\hat{\varphi}\big)\cos^q\theta \qquad (2)$$

Finally, the wave incidence angle on the surface of the RA can be particularly relevant in the context of mechanical beam scanning and multi-beam. The delay introduced by the array unit cell is affected by this angle to a certain extent, which causes slight alterations in the phase response of the array for each feed position. The impact of this effect is evaluated in Section IV, where the discrepancies between a physical layout and a phase-only solution are studied for multiple feed positions.

III. Geometry Analysis

A compact Ka-band at 29.5 GHz is studied under two different geometries. A rectangular panel with dimensions $D_x = 232$ and $D_y = 171$ mm is considered, which correspond to roughly 22.8 and 16.8 λ. The scanning and feed

displacements are performed in the XZ plane. An F/D ratio of 0.4 is selected for the two cases, with $D = D_y$ and F being defined for each geometry as shown in Fig. 1 and Fig. 3.

The panel is illuminated using an x-polarized low-gain feed e.g., an open waveguide. For the feed model in (2), q is set to 2.1 and E_0 is selected so that the overall feed gain is 7.5 dBi. For a centered feed position pointed orthogonally towards the RA panel, this results in an illumination taper on the y-axis of approximately 12 dB.

A. Focal Arc Displacement

As depicted in Fig. 1, the feeding element is displaced from its reference position a certain angle θ_f along an arc, while being pointed towards the panel center. By moving the feed out of focus, the resulting radiation diagram inevitably degrades in terms of gain, beamwidth and SLL. However, this also produces a natural shift in the direction of the main lobe. If the radiation angles are not too oblique, and the new feed position lies in the vicinity of the focus position, the shift in θ_0 is roughly the opposite to that of θ_f. Note that this type of feed displacement ensures that the orientation of the feed is always towards the same point on the reflector surface. As a result, the surface illumination is very similar, and the majority of the aperture is shared between all feed positions.

For this study, the reference feed position is set at $\theta_f = 0$ deg, and the RA phase response is calculated to generate a beam in the specular direction, i.e. $\theta_0 = 0$ deg. By designing the panel around specular reflection, the natural beam deviation is efficiently exploited. The selection of the focus position results in a symmetrical scanning behavior for any pair of angles $\pm\theta_0$. Fig. 2 shows the calculated radiation diagram for a range of feed positions, and the gradual degradation in the main lobe for more oblique angles. The close relation between θ_0 and θ_f can also be observed.

Due to its conceptual simplicity and wide scanning range, examples of this configuration can be found in the literature [6]. Despite this, one major disadvantage of this approach that is not reflected in Fig. 2 is the blocking caused by the radiating element and its support structure, which is likely to significantly degrade the central beams. This is mitigated in some works by using a non-centered reference feed position and targeting only either the positive or negative θ_0 range [7]. Blocking is thus reduced for all but the near-broadside beams, at the cost of a reduced scanning range. Configurations based on focal arc displacement also require a complex railing system to enable the feed movement and tilting, which is likely to aggravate the blocking issue.

B. Linear Displacement

The second geometry in this study consists of a linear movement of the feed from the focus position, as shown in Fig. 3. This reduces the complexity of the feed displacement system, as there is no need for tilt control or arcing of the feed path. There are more design parameters in this configuration: the tilt angle of the feeds θ_f, and the tilt angle of the feed displacement line τ. The case with $\tau = 0$ if of particular interest. The reason is that the feed movements become parallel to the RA plane. Thus, they can be replaced by in-plane displacements of the reflector panel itself. Since they involve no active RF components, these are significantly simpler to implement. Notice that the surface point that the feed is oriented towards changes with the feed's position. This translates to a partial aperture overlap between feeds. Optimization techniques may exploit this fact by selecting the phase response of each point in the aperture so that it favors certain feed positions based on their illumination levels.

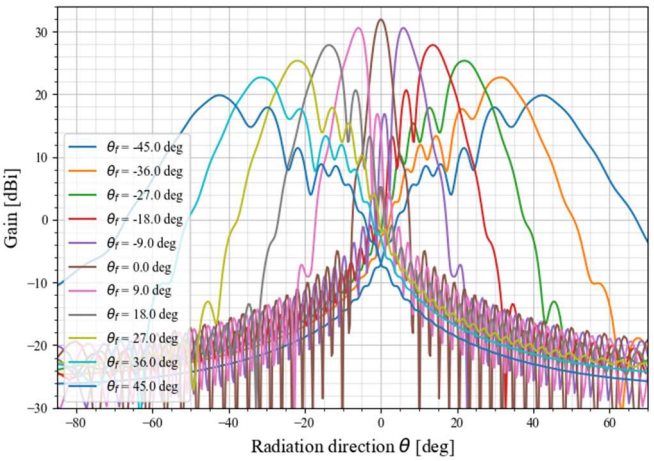

Fig. 2. Radiation pattern cut at $\varphi = 0$ for multiple feed positions along the focal arc.

First, the $\tau = 0$ case is studied in detail. To do so, the scanning performance of this configuration is evaluated at several feed tilt angles θ_f. For every angle, the valid range of feed positions along the x-axis is calculated. Valid positions are those that achieve a field taper at $\pm D_x/2$ of at least 10 dB, since lower values would result in high spillover losses. The middle point of this range is used as the reference feed position for calculating the phase response distribution in each case, which is designed for a main output beam at $\theta_0 = 25$ degrees. This ensures that there is no significant blocking for any feed position.

The radiation pattern is calculated for the ranges of feed positions in the same way as the focal arc configuration. Fig. 4 shows the scanning performance achieved in each case. Note that, for the purpose of clarity, only the main radiation direction and its associated gain are shown for each feed position in this case. These results show that the achievable gain and scanning range deteriorates the higher the feed tilt angle is. The reason is that higher θ_f values translate into a worse illumination taper,

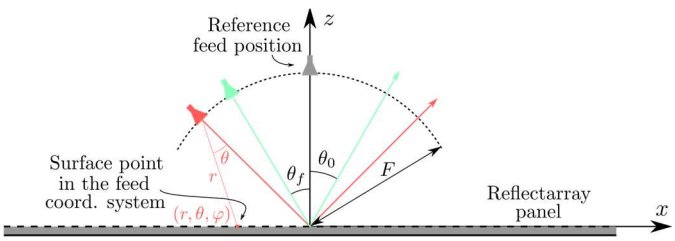

Fig. 1. Geometry for focal-arc displacement mechanical scanning.

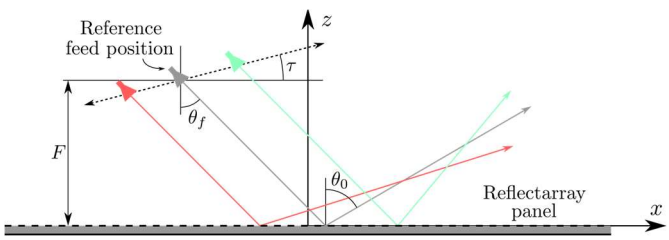

Fig. 3. Geometry and defining parameters for a scanning geometry based on linear feed displacements.

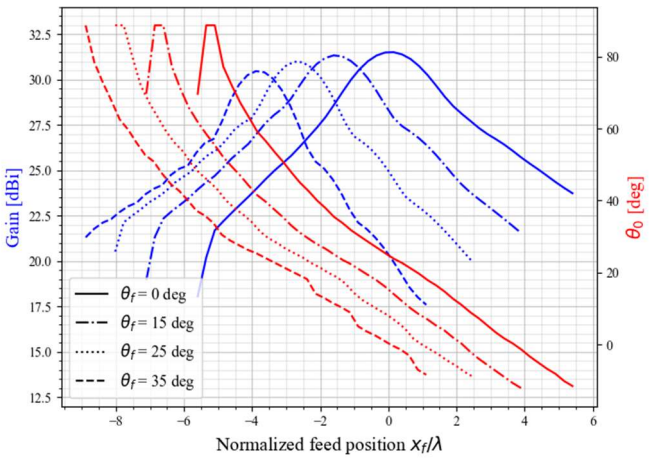

Fig. 4. Main radiation direction and gain resulting from in-plane feed displacements along the x-axis, for several feed tilt angles θ_f.

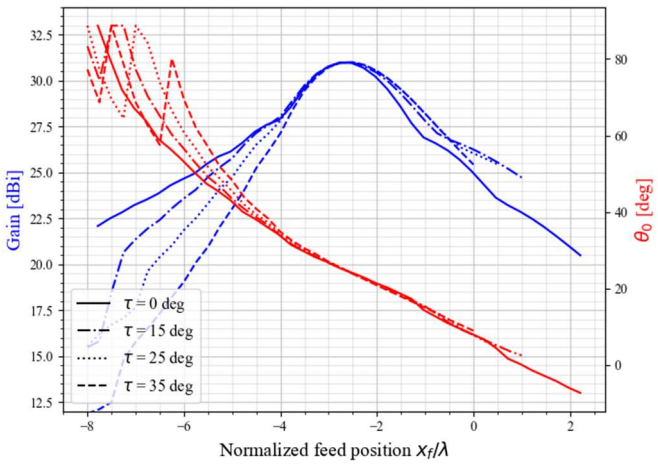

Fig. 5. Main radiation direction and gain resulting from feed displacements oblique to the reflectarray plane, for a constant feed tilt angle of $\theta_f = 25$ deg and multiple feed axis angles τ.

and thus reduced efficiency. For example, for the case of $\theta_f = 35$ deg, the taper in the y-axis is only around 5.8 dB. This issue would be partially compensated by a different choice of a feeding element and should therefore be a small concern if the tilt angle is kept relatively low. The main benefit of a feed tilt is that it mitigates or negates the blocking that would otherwise affect the beams near broadside.

Next, the effects of tilting the feed axis are evaluated. To do so, θ_f is fixed at 25 degrees, and the same feed reference position as before is used. The beam pointing for the design of the phase response of the array is also set to 25 degrees. Fig. 5 shows the gain and main radiation for four τ values. It can be observed that increasing the tilt angle results in a faster gain drop-off as the feed leaves the focus position. In a similar way to what happened for $\tau = 0$, this is caused by a degraded illumination efficiency. When the feed is located at $x_f < x_{ref}$, it gets closer to the reflector panel and thus the taper efficiency degrades, while for $x_f > x_{ref}$ positions the feed is farther away and thus it is the spillover efficiency that decreases. Contrary to the $\tau = 0$ case, it is not possible to fix the illumination efficiency by changing the feeding element. The reason is that the effective illuminated area changes for different feed positions at any $\tau \neq 0$ value.

From these results, it can be concluded that introducing a tilt to the feed displacement axis has no clear advantage from a beam scanning perspective: it introduces significant complexity to the mechanical implementation, while also deteriorating the beam scanning performance and increasing the volume of the solution. It does however have a major advantage as a multi-beam solution. In this case, the configuration would not consist of a single movable feed, but rather a set of feeds at fixed positions along the axis, thus eliminating the mechanical complexity. It may also be preferred over the $\tau = 0$ configuration, as the tilt to the feed axis should alleviate any blocking that feeds located at higher x_f positions may cause to beams generated by feeds at lower x_f values. Lastly, the degradation in illumination efficiency could also be resolved in a multi-beam scenario by selecting multiple different feeding elements. However, this would also increase the cost and complexity of the design.

IV. Reflectarray Design

A. Cell Characteristics

The unit cell geometry selected for this design is represented in Fig. 6. It consists of three parallel dipoles printed on a metal-backed substrate. This design has been proven by previous works [8] to provide a wide phase response range, while showing high stability to the incidence angle.

The chosen substrate is DiClad 880, with a permittivity of $\epsilon_r = 2.3$, loss tangent of 0.005 and a thickness of 0.762 mm. The periodicity on both axis is set to 4.07 mm (about 0.4 λ). The dipole width W is set to 0.5 mm, S to 1.36 mm and α to 0.72. The cell response is analyzed under local periodicity conditions [4], resulting in the curves shown in Fig. 7. The phase response covers 360 degrees, with losses staying below 0.5 dB. The response also shows high angular stability, which should make the phase-only designs shown above highly accurate.

B. Layout Design

Using the unit cell described above, a RA layout of 57 by 42 elements is designed, for a total D_x and D_y size equal to the ones considered in the phase-only study above. The selected configuration is the linear-displacement geometry from before, with $\theta_f = 25$ degrees and $\tau = 0$. The L dimension is selected for each cell considering the real incidence angle from the reference feed position. Thus, the phase response of the entire panel should match the ideal phase-only approximation at the reference position –neglecting losses introduced by the cell–. However, other feed positions will experience small discrepancies as a result of the difference in incidence angles.

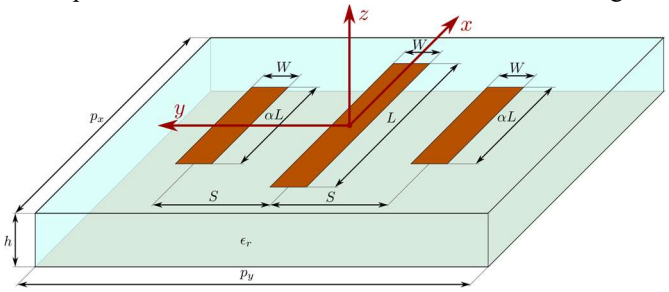

Fig. 6. Sketch of the reflectarray unit cell used for this design. The center-dipole length L is selected for each desired phase response.

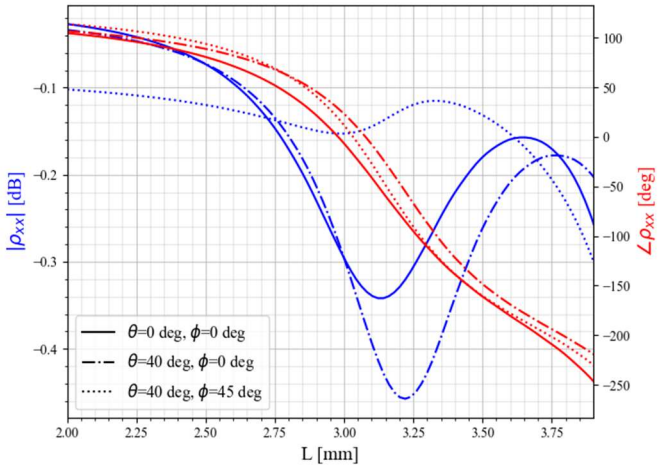

Fig. 7. Unit cell ρ_{xx} response under different incidence angles.

The response of the entire layout is then calculated for a range of feed positions, considering the real incidence angles for each cell and feed position combination. The resulting reflected tangential fields are used to calculate the far-field copolar components, with the $\varphi = 0$ radiation pattern cuts being represented in Fig. 8. Note that these curves reflect the attenuation introduced by the unit cell as well as any discrepancy caused by the variation in the incidence angles. The patterns obtained using ideal phase distributions are also shown in the same Figure. Differences between the two solutions are negligible in both gain and radiation direction for beams pointed near the reference direction of $\theta_0 = 25$ degrees. Beams at the edges of the shown scanning range show a slight deviation of less than 2 degrees between the ideal scenario and the full-wave simulation of the cell responses.

V. Conclusions

Two common RA-based beam scanning geometries are studied. Their natural scanning performance is evaluated before any optimization is applied to the design of the RA phase response. Focal arc feed displacement shows a symmetrical scanning range with a simple configuration. However, the mechanical implementation is costly, and blocking is a major issue. In comparison, planar feed displacements are found to achieve comparable ranges, while enabling simpler in-plane reflector movements. Blocking can be mitigated by introducing sufficient tilt to the feed. Finally, oblique feed displacements are found to decrease the illumination efficiency when far from the focal point, while also complicating the mechanical structure. However, they can be an interesting choice for multi-beam designs, which could mitigate the downsides of this geometry.

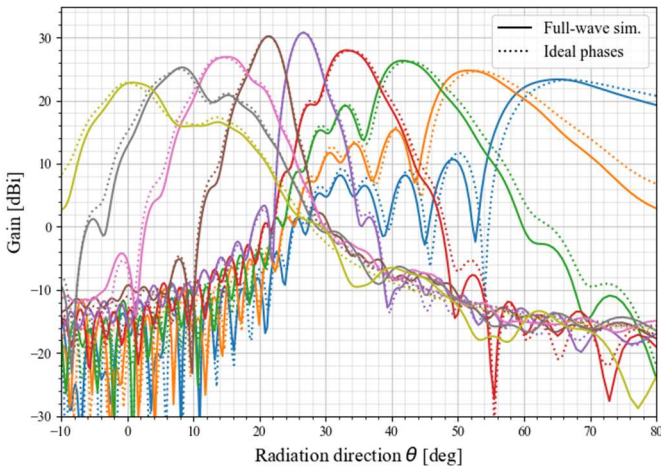

Fig. 8. Comparison of radiation pattern cuts ($\varphi = 0$) between an ideal phase distribution and a real layout response, using in-plane panel movements. The purple curve is associated to the ref. position.

Next, the effects of the incidence angle are studied for these geometries. A layout is designed for a collimated beam in one specific configuration using a unit cell with high angular stability. Its natural scanning capabilities are evaluated while considering the actual incident angles for each feed position, and they are compared to an ideal case with a fixed phase distribution. Discrepancies are found to be minimal between the ideal phase-only model and the real layout response.

Acknowledgment

This work was supported in part by Ministerio de Ciencia e Innovación and Agencia Española de Investigación within the project (PID2020-114172RB-C21 / AEI / 10.13039 / 501100011033); by Gobierno del Principado de Asturias under project AYUD/2021/51706; and by Ministerio de Educación y Formación Profesional under grant FPU20/07267.

References

[1] T. Li, E. Murugesan and Z. N. Chen, "Ka-band Mechanically Beam Scanning Bifocal Reflectarray Antenna with Optimized Phase Distribution," 2020 IEEE International Conference on Computational Electromagnetics (ICCEM), 2020, pp. 209-210, doi: 10.1109/ICCEM47450.2020.9219497.

[2] E. Martinez-de-Rioja, J. A. Encinar, A. Pino and B. Gonzalez-Valdes, "Design of Bifocal Dual Reflectarray Antennas in Ka-band to Generate a Multi-Spot Coverage from Geostationary Satellites," 2019 13th European Conference on Antennas and Propagation (EuCAP), 2019, pp. 1-5.

[3] E. B. Lima, S. A. Matos, J. R. Costa, C. A. Fernandes and N. J. G. Fonseca, "Circular Polarization Wide-Angle Beam Steering at Ka-Band by In-Plane Translation of a Plate Lens Antenna," in IEEE Transactions on Antennas and Propagation, vol. 63, no. 12, pp. 5443-5455, Dec. 2015, doi: 10.1109/TAP.2015.2484419.

[4] J. Huang and J. A. Encinar, *Reflectarray Antennas*. Hoboken, NJ, USA: Wiley, 2008.

[5] Y. T. Lo and S. W. Lee, "Antenna Handbook", vol. 1. Van Nostrand Reinhold, 1993, ch.1, pp. 28-29.

[6] G. Wu, S. Qu and S. Yang, "Wide-Angle Beam-Scanning Reflectarray With Mechanical Steering," in IEEE Transactions on Antennas and Propagation, vol. 66, no. 1, pp. 172-181, Jan. 2018, doi: 10.1109/TAP.2017.2775282.

[7] G. -B. Wu, S. -W. Qu, S. Yang and C. H. Chan, "Low-Cost 1-D Beam-Steering Reflectarray With ±70° Scan Coverage," in IEEE Transactions on Antennas and Propagation, vol. 68, no. 6, pp. 5009-5014, June 2020, doi: 10.1109/TAP.2019.2963572.

[8] Á. F. Vaquero, M. Arrebola, M. R. Pino, R. Florencio and J. A. Encinar, "Demonstration of a Reflectarray With Near-Field Amplitude and Phase Constraints as Compact Antenna Test Range Probe for 5G New Radio Devices," in IEEE Transactions on Antennas and Propagation, vol. 69, no. 5, pp. 2715-2726, May 2021, doi: 10.1109/TAP.2020.3030969.